J. Kor. Powd. Met. Inst., Vol. 21, No. 2, 2014
DOI: 10.4150/KPMI.2014.21.2.155

PM Trend

Planetary Ball Mill Process in Aspect of Milling Energy

Huynh Xuan Khoa, Sunwoo Bae, Sangwon Bae, Byeong-woo Kim[a], and Ji Soon Kim*
School of Materials Science and Engineering,
[a]School of Electrical Engineering, University of Ulsan, 93 Daehak-ro, Nam-gu, Ulsan 680-749, Korea

유성밀 프로세스와 밀링에너지

Huynh Xuan Khoa · 배선우 · 배상원 · 김병우[a] · 김지순*
울산대학교 첨단소재공학부, [a]울산대학교 전기공학부

1. Introduction

Milling is a core fabrication process in powder technology. Especially the high-energy milling technology is being frequently used in energy-intensive process like mechanical alloying, mechanical activation and mechanochemistry, etc. Planetary ball mill is a representative high-energy mill together with shaker mill, stirred mill and vibration mill. Since milling condition strongly affects the property of milled powder materials, it should be controlled by changing the milling balls, the milling vial, the geometry of mill, and the rotation speed etc. to obtain an end product with desired characteristics. Milling with large, high density balls and higher rotation speed seems to provide materials with higher impact energy in comparison with small, low density balls and lower rotation speed. It is important to have an understanding the relationship between the milling process variables and the characteristics of final powder products. Many researchers have reported already their results and theories in such aspects. Attempts to modeling the ball mill process have been done in the last decades [1-14]. Burgio *et al.* [1] has established the fundamentals of mathematic model for determining the impact velocity of the ball and the energy transferred to powder. Padella [6] reported the results from experiments in which the energy transfer was intentionally controlled to form either intermetallic compound or amorphous phase of Pd-Si system. Research works to establish a milling map have pointed out the importance of determining which milling parameters have to be employed in order to obtain a particular final product.

This paper reviews the theories of milling energy in planetary ball mill process based on the collision model.

2. Planetary Ball Mill: A Representative High-energy Mill

Planetary ball mill is a representative high-energy mill especially used for energy-intensive process like mechanical alloying, mechanical activation or mechanochemistry, etc. The term “high-energy” is often used to differentiate from “low-energy” conventional drum or ball mills. The name of planetary mill is derived from its unique kine-

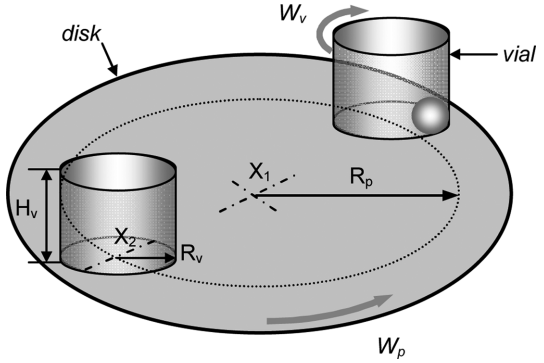

Fig. 1. Schematic illustration of planetary disk with movement in a counter direction of vials: R_p and W_p - revolution radius and speed, R_v and W_v - rotation radius and speed, H_v - vial height.

*Corresponding Author : Ji Soon Kim, **TEL:** +82-52-259-2244, **FAX:** +82-52-259-1688, **E-mail:** jskim@ulsan.ac.kr

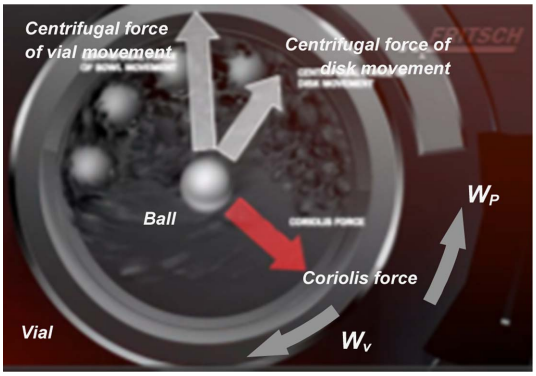

Fig. 2. A snapshot of the ball motion inside the planetary ball mill with set of forces on a ball from video introducing Pulverisette 6 classic line – FRITSCH GmbH [15].

matics. As shown in Fig. 1, the grinding vials are mounted on a revolving disk, rotate on its axis (X_2) with a rotation speed W_v, the disk also revolves on its axis (X_1) with a revolution speed W_p. The direction of vials is normally counteractive to the revolving disk to generate higher impact energy of balls [15].

Due to such planetary movement, each ball filled in vials is not just subjected to the gravitational force as with traditional ball mills. Additional coriolis and centrifugal force (Fig. 2) increase further kinetic energy of the grinding components up to 100 times the gravitational force [16]. Through such a high kinetic energy, materials loaded in mill are quickly and effectively comminuted by impact, frictional and shear forces resulting from ball-to-wall and ball-to-ball collisions. Of commercially available planetary ball mills, the Fritsch Pulverisette mills [16], RETSCH planetary ball mills [17] and AGO-2 mills [18] are most frequently used. The Pulverisette 7 premium line is known to generate a centrifugal acceleration of 95 g (g=9.81 m/s^2) [19] and the AGO-2 mill 60 g [2]. The characteristics of planetary ball mills are high impact velocities and high impact frequencies of the milling ball. The impact velocities for various mills have been reported to reach to 12 m/s for a SPEX shaker mill, 14 m/s for Simoloyer, 5 m/s for planetary ball mill and Attritor, and below 5 m/s for ball mill [3]. The impact frequency of a SPEX mill had been calculated to be 1020/min (or 17/s) Maurice and Courtney *et al.* [4] and 17-19/s for the planetary ball mill (Fritsch Pulviresette P5) at a rotation speed of 350 rpm [20]. These two mills are therefore being used widely as representative high-energy mill.

3. Previous Reports on Planetary Ball Mill Theory

Many of researchers had been interested in the phenomena occurring in the milling container such as the ball motion, the model of ball-to-wall and ball-to-ball collisions, the frequency of the collisions, the deformation of the powder trapped between collision bodies, etc. They had tried to correlate the processing variables and the milling energy.

Attempts of modeling the ball milling process have been very active in the last two decades. The aim of constructing a model was mainly for predicting the formation of the desired products by adjusting the milling parameters appropriately and making the design of mechanical alloying process possible. Firstly, Maurice and Courtney [4] attempted to define the basic geometry, mechanics and physics of the powder-workpiece interaction for several milling devices such as attritor, vibratory mill and horizontal ball mill, since these information allow pertinent parameters of the process (e.g. impact velocity, powder material volume impacted, time between impacts, etc.) to be identified in terms of machine characteristics and process operating parameters. The numerical calculations showed that the phase transition is governed by only the injected shock energy. Burgio *et al.* [1] attempted to correlate the milling operative conditions and the characteristics of the end product. Using the model based on the *FRITSCH* Pulverisette P5 planetary ball mill, they derived the kinematic Eq.s describing the velocity and kinetic energy of a ball in a vial and the collision frequency. From these basic parameters, the energy transfer to the powder during milling process could be calculated and an energy map was constructed to allow for defining the milling conditions under which either intermetallics or amorphous phase are formed. The collision model developed by Burgio was modified by Magini [5]. In order to analysis the hit mechanism, the velocities of the balls inside the vials were estimated, using the difference between the potential energies before and after the collision event of a ball on a flat surface, calculated the kinetic shock energy released by the ball into the powders. Le Brun *et al*. [7] used a video recorder to study the ball movement in a planetary mill and described an "impact plus friction" regime. Trajectories of balls in the

mill were calculated in order to predict the operative modes of a planetary ball mill. The angular velocity ratio (R, a ratio of rotation speed of the vial and revolution speed of the disk) is useful in the description of the kinetics of the mill. Based on the calculation of the movement of a ball, they indicated that three different types of trajectory are possible. These three different milling modes appear when the ratio of the milling velocities is modified and are termed "chaotic" (pure impact) for $R < R_{limit}$, "impact + friction" for $R_{limit} < R < R_{critical}$ and "friction" for $R > R_{limit}$. The study suggested that a mill could be designed for specific purposes depending upon the value of R. Pure impact is obtained for $R = 2.25$, whereas high friction results from values close to $R_{critical}$.

Gaffet [8-10] suggested through more rigorous analyses that the power of ball impact rather than the kinetic energy or frequency might determine the characteristics of end products and the efficiency of the milling process. These models, however, overlooked some important kinematic parameters like the angular variation of impact velocity in determining the effective amount of power/energy transferred to the powder particles during a given collision event. In this regard, Besset *et al*. [11] proposed that the impact velocity might be experimentally determined from the size of indentation on a metallic surface. Magini and Iasonna [12], Iasonna and Magini [13] and Magini *et al.* [14] considered the same kinematic conditions proposed by Burgio *et al.* [1], and calculated the energy transferred per impact to compare the latter with the experimentally determined electrical/mechanical power consumed. In spite of such an elegant approach, the analysis did not yield an optimum condition of milling in terms of power/energy for a given mechanical alloying condition. Watanabe *et al.* [15] simulated the kinematics and related them with the trajectory of ball motion for a various ball mill devices using Kelvin's dashpot-spring model. The analysis as well as the photographic observation of ball trajectory suggested that the relative direction of rotation between the disk and vial (i.e. parallel and counter rotation) determines the nature of ball trajectory, i.e. cataracting and cascading motion, respectively. Chattopadhyay *et al.* [21] presented a kinematic analysis in terms of a single Cartesian reference frame for both the rotating disk and vial. The model explicitly defined the role of milling parameters in determining the criterion for the detachment of ball from the rotating vial wall prior to impact, so that the detachment angle never assumes an unrealistic value in the subsequent analysis.

Recently, Mio *et al.* [22-24] performed a set of experiments to study effects of the rotational direction of a pot in a planetary ball mill and its speed ratio against revolution of a disk on the specific impact energy of balls calculated from the simulation on the basis of the Discrete Element Method (DEM). The specific impact energy increases with an increase in the rotation-to-revolution speed ratio in the initial stage and then falls around the critical speed ratio, which can be calculated by the balance Eq. based on the centrifugal forces acting on a ball due to the combination of the rotation and revolution. The highest value in the specific impact energy of balls during milling could be achieved effectively around this critical speed. This critical speed would, therefore, be a key condition in milling for designing suitable and optimum mechanical milling performance. The scale-up method for the planetary mill was also established by evaluating the impact energy. The impact energy is proportional to the cube of the diameter of the pot, the depth of the pot and the revolution radius of the disk, respectively. When the planetary mill is scaled-up in geometrical similarity, the impact energy of the balls is proportional to 4.87 power of the scale-up ratio. Lu *et al*. [25], based on the kinematics of ball motion, described the collision frequency and power. They derived the normal impact forces and the effective power from analysis of collision geometry. The impact angle of the milling ball ranged from 90 to 0 with the variation in the angular velocity ratio. The ideal values of the normal impact force and tangential force could be obtained. When the dynamic parameters of the planetary ball mill were given, the highest impact energy could be obtained for the optimal value of angular velocity ratio. The optimal ratio was found to be 1.15 at 800 rpm.

4. Processing Variables in Planetary Ball Mill Process

The planetary ball mill process involves loading of the powder particles with the grinding medium in a container and subjecting them to heavy deformation. Processing variables can be divided in three groups as follows:

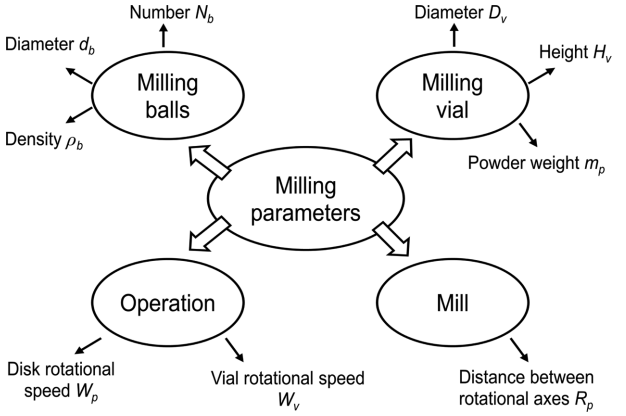

Fig. 3. High-energy milling parameters of a planetary ball mill using cylindrical vial [26].

The milling device:

Type of mill: kinetic factor (W_v/W_p), geometrical factor (R_p/R_v)

Milling container: diameter (D_v), height (H_v)

Operation:

Milling speed (W_p), milling time (t), milling frequency (f) (or intensity)

Type (ρ_b), size (d_b) and number (N_b) of balls, filling ratio (n_v)

Ball-to-powder weight ratio (BPR)

Others:

Milling atmosphere, process control agent, temperature

The main difficulty in constructing a mathematical model arises from the numerous milling parameters that describe the energetics of the high-energy milling process. Rojac *et al.* [26] have summarized the milling parameters for a planetary mill using cylindrical milling vial (Fig. 3). Nine parameters from the first and second groups are given to describe the process and can be involved in establishing the relation with the milling energy. The purpose of establishing the mathematical model is to correlate the milling parameters with the ball-impact energy as well as with the frequency of ball-to-wall and ball-to-ball collisions, thereby the relation of the milling energy and processing variables can be determined.

5. Correlation of Processing Variables with the Milling Energy

5.1. Determination of the absolute velocity(v_b) and the kinetic energy of a single ball

As illustrated in Fig. 2, the powder is ground by two colliding balls and/or a ball colliding against the vial wall. Some works regarding the kinematics of the ball motion and a calculation of the absolute velocity have been reported by Burgio [1], Abdellaoui and Gaffet [9]. The Eq. used for calculating the absolute velocity of the balls is as follows (Eq. A.10 of ref. [1])

$$v_b = [(W_p R_p)^2 + W_v^2 (R_v - d_b/2)^2 (1 - 2W_v/W_p)]^{1/2} \quad (1)$$

This Eq. points out that the absolute velocity of a ball basically depends on kinetic factor (W_v/W_p) and geometrical factor (R_p/R_v). If these factors were fixed as in a mill with given geometry, the absolute velocity of a ball impacting the vial wall:

$$v_b = K_b W_p R_p \quad (2)$$

K_b is a geometrical coefficient depending on the geometry of the mill. For a planetary mill, it is ~ 1.06 for a point ball and ~ 0.90 for a ball with diameter of 10 mm. Because of simplicity of the Eq. (2) it is usually used to calculate the kinetic energy of the ball.

When the ball is launched as shown in Fig. 2, it possesses the kinetic energy. In classical mechanics, the kinetic energy of a non-rotating object of mass m traveling at a speed v is ½ mv^2. So the kinetic energy involved in the collision is then given by:

$$\Delta E = (1/2)\, K_a\, m_b\, v_b^{\,2} \quad (3)$$

where m_b is the mass of a ball and K_a is a constant describing the property of collision. K_a is zero for perfect elastic collisions (no energy transfer) and 1 for perfect inelastic collisions. If the balls were covered in a form of coating with powder, the collisions are almost perfectly inelastic, so that K_a is often 1. It was also verified that in the early milling stages the fraction of kinetic energy transferred to the powder is practically equal to the total energy involved in the collision event. The energy transferred to the powder per ball and collision event is then given by:

$$\Delta E = K_c m_b W_p^{\,2} R_p^{\,2} \quad [joule/hit] \quad (4)$$

where $K_c = (1/2) K_a K_b^2$; m_b [kg], W_p [$rpm = 2\pi/60$ *rads/sec.*], R_p [m]

The analysis of the collision previously described allows to assume that the Eq. (4) really represent the energy given to the powder in a real milling process, at least as long as the collision is considered to be in elastic.

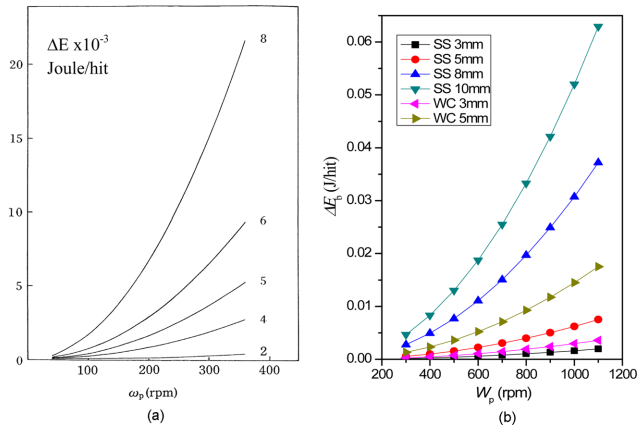

Fig. 4. Energy dissipated per hit versus the rotation speed of the planetary ball mill (Fritsch "Pulverisette 5" [11] (a) and AGO-2 (b)).

The Eq. (4) reveals that the energy transferred to the powder depends on the ball mass and the rotation speed of the mill because revolution radius (R_p) is fixed for a given milling device. Fig. 4 represents the energy released per hit as a function of the rotation speed of the mill and the mass of the ball for the given materials and the diameter. The values were calculated using Eq. (4) for Fritsch "Pulverisette 5" [16] and AGO-2 mill for various stainless steel balls and WC balls. The balls with large diameter or high density can provide higher impact energy at the collision event. The magnitude of the energy transfer occurring during a collision event has been reported as ranging the order of 10^{-2} J/hit.

In the case that N_b balls are used in the experiment, Eq. (4) should be modified in order to account for the degree of filling of the vial, by considering a yield coefficient $\varphi_b < 1$.

The energy ΔE_b^* dissipated by one ball in a system with N_b ball is given by:

$$\Delta E_b^* = \varphi_b \Delta E_b \tag{5}$$

The φ_b can be defined either by accurate mathematical modeling or by means of experimental measurements. It's convenient to express φ_b as a function of a parameter n_v:

$$\varphi_b = (1 - n_v^e)$$

Most of the details were described in [1], φ_b is close to 1 for 1/3 filling of the vial and ε is a parameter depending on the ball diameter. The degree of filling, n_v, defined as $n_v = N_b/N_{b,tot}$. Where $N_{b,tot}$ is the total number of balls necessary to completely fill up the vial so that no ball movement is possible.

5.2. Energy transfer per unit of mass and milling map

We experience frequently that in the early stage of milling most of the powder adheres to the surface of the balls and the vial walls, especially in case of ductile metallic powder material systems. As far as the quantity of powder material trapped in between a ball and the container wall during a collision is concerned, the energy transfer per unit of mass is given in [20]

$$\Delta E/Q_{max} = (7.66 \times 10^{-2}\, R_p^{1.2} \rho^{0.6} E^{0.4})\, d_b W_p^{1.2}/\sigma \tag{6}$$

where Q_{max} is the maximum quantity of trapped material in the radius of the circular area at the maximum of compression, $R_{h,max}$, and is given by

$$Q_{max} = 2\sigma\pi R_{h,max}$$

ρ is the density of the balls used ($\rho_{stainless\ steel} = 7.64 \times 10^3$ kg/m^3, $\rho_{wc} = 15.82 \times 10^3$ kg/m^3), E is Young's modulus of the ball used, it is 2.11 and 7.2×10^{11} N/m^2 for stainless steel and WC ball, respectively. σ, the adhering powder surface density, can be estimated by measuring the weight of the powder coating the balls, and the factor "2" takes into account that twice the surface density (ball and vial surfaces) must be considered.

Magini *et al.* quantified material trapped in the collision event to evaluate the energy transfer per unit of mass. Based on this relation, an energy map for milling of Pd-Si system was established in order to find out the relationship of milling condition and characteristics of the

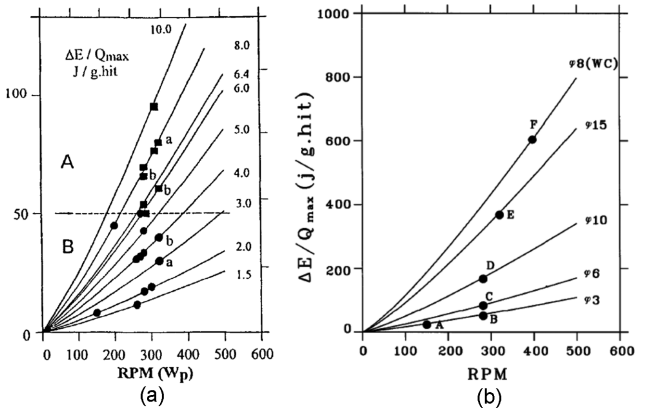

Fig. 5. (a) The energy map for the Pd-Si system, letter a = $Pd_{86.5}Si_{13.5}$ and letter b = $Pd_{83}Si_{17}$, the rest is $Pd_{80}Si_{20}$ [20] and (b) The energy map for mechanical alloying of Mo-Si mixture[27].

end-products [20].

The energy map of Fig. 5(a) shows a predictive capability for any experiment carried out on the Pd-Si system in any milling condition. The continuous lines are $\Delta E/Q_{max}$ - $d_b W_p$ relationship of Eq. (6) with d_b from 1.5 to 8.0 mm. A threshold value of 50 J/g·hit separates the energy map into two regions. Milling with energy above the threshold, amorphous phase was formed, but below this value only intermetallic phase could be found.

Liu and Magini [26] also established the milling map for mechanical alloying of Mo-Si system as shown in Fig. 5(b). The map reveals that in case of milling with the lowest energy input, Condition A, no reaction occurred. By increasing milling energy from Condition B to E, intermetallic compounds with different phases were formed. According to the XRD results, the high temperature phase β-$MoSi_2$ was formed as milling with lower milling energy (B to D conditions), while the low temperature phase α-$MoSi_2$ was mainly included in the end product with the highest milling energy.

5.3. Power consumption

The Eq. (4) gives the energy transferred to the powder during a single collision event. Multiplying this energy by the number of events per unit time, i.e., by the frequency of the hits, we obtain the power absorption. The collision frequency, f, for a single ball can be written as follows [1].

$$f = K(W_p - W_v)/2\pi = KkW_p = K_v W_p \quad (7)$$

The value of K depends upon the ball diameter and can be evaluated to be approximately 1.5 for ball diameters of 8-10 mm. The k is the kinetic factor, the ratio of W_v/W_p, that is 1.15 and 1.65 for the Fritsch "Pulverisette 5" and AGO-2, respectively. In the experiments that the vials were filled at a low level, the reciprocal hindering of the N_b balls is negligible and the total collision frequency f_t is given by

$$f_t = fN_b$$

The calculated power consumption is thus given by

$$P_{cal} = \Delta E f_t$$
$$P_{cal} = (1/2)\, K_a K_b K_v\, m_b W_p^3 R_p^2 N_b \quad (8)$$

If vial were filled at a high level, the reciprocal hindering coefficient of the N_b balls, φ_b, has to be considered in calculating the power consumption.

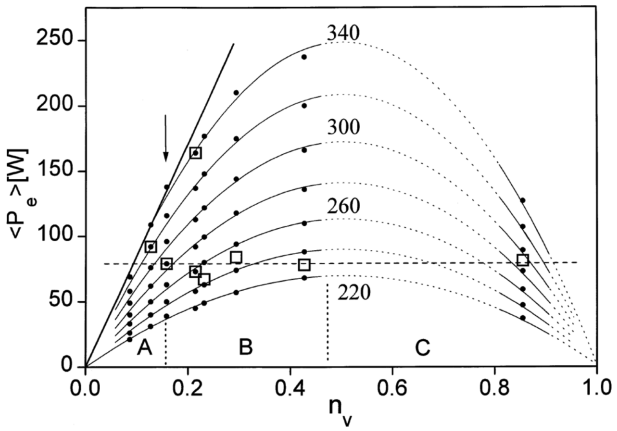

Fig. 6. Milling map showing the P_e-n_v relationship with typical planetary mill rotation speeds [14].

$$P_{cal} = \varphi_b \Delta E f_t$$
$$P_{cal} = P^* \varphi_b m_b W_p^3 R_p^2 N_b, \text{ [W]} \quad (9)$$

with P^* includes $(1/2)K_a K_b K_v$

Eq. (9) is the power consumption during milling predicted by the collision model. It can help to set up the suitable milling condition in order to obtain a desired end product.

Fig. 6 shows the power absorption as a function of the filling of the vial and the rotation speeds of the planetary mill [14]. The power values on the vertical axis indicated by dots are the measured values for typical rotation speeds. It can be seen from Fig. 6 that three different efficiency regions exist. In the first region(A) the power consumption increases linearly with the filling up to about $n_v \leq 0.18$ (arrow). In this region there is no reciprocal hindering of the balls, the yield coefficient φ_b is nearly 1. When $n_v > 0.18$, the P-n_v relation deviates from linearity (region B). This means that above a certain level of filling, the balls hinder each other and thereby the energy transfer process becomes less effective than expected ($\varphi_b < 1$). In other words the efficiency with respect to the charge decreases. Beyond the peak ($n_v \approx 0.5$), the power consumption decreases in absolute value, region C, and tends towards zero ($\varphi_b = 0$).

The horizontal dash-line shows equi-power consumption. On this line, the power consumption is constant for any different n_v and W_p. Due to the constant power consumption, it is expected that the same end product might

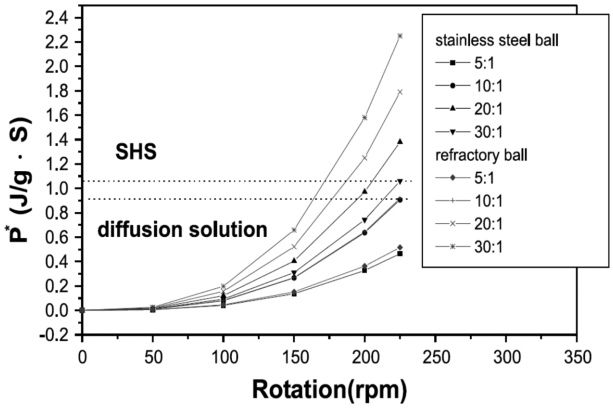

Fig. 7. The milling map of $MoSi_2$ at different conditions [28].

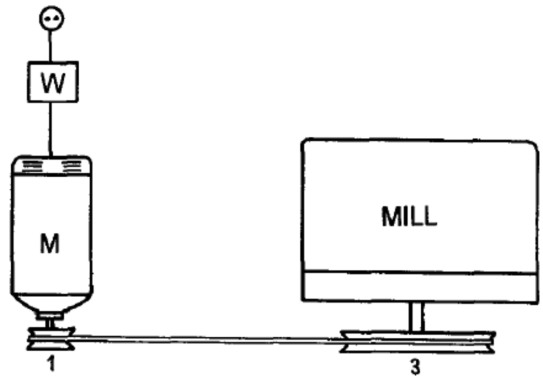

Fig. 8. Schematic illustration of the electrical power measurement system for planetary ball mill [13]. (W – the power meter, M – the electric motor)

be obtained even from different milling conditions for the same milling time. To confirm above consideration, they performed the milling of Ni-CuO powder mixture at nearly equi-power consumption by varying both n_v and W_p. After the milling with P_e of 79W (n_v = 0.16, W_p = 280 rpm), 78W (n_v = 0.43, W_p = 230 rpm) and 81W (n_v = 0.86, W_p = 290 rpm) for 7h, the XRD-patterns showed an indistinguishable shape. By increasing the level of power consumption at twice (165W with n_v = 0.21, W_p = 340 rpm) the equi-value, the reaction proceeded much faster and was completed in less than a half the milling time (for more details see [14]).

Zhang and Liu [28] have performed a number of experiments on the Mo-Si system varying W_p, ball-powder weight ratio and ball medium, as shown in Fig. 7. This indicates that the energy map of the figure defines the range of values (P = 1.06 J/g·s) above this SHS formation mechanism will be attained and of the value (P = 0.917 J/g·s) below which diffusion solution formation mechanism will be attained. The map establishes a predictive capability for other experiments carried out on the Mo:2Si system in different milling conditions.

5.4. Measuring the power consumption and milling energy

With collision model as described in Fig. 2, the power consumption can be calculated by Eq. (8). The question is that the order of magnitude of the microscopic event is correct and it should be revealed at macroscopic level for convenience. That is, the calculated values should be confirmed by the experimental measurement. Every milling device consumes electrical power for milling operation. In this sense it is simple and convenient to measure the electrical power absorption during milling process such as Fig. 8 suggested by Magini *et al*. [13, 14].

They performed a series of milling experiments using Fritsch "Pulverisette 5" equipped with two stainless steel vials of 250 cm^3 and measured power consumption by a power meter (indicated by W in Fig. 8). First, the energy absorbed by the mill charged with two empty vials was measured. Then, the vials were filled with a given number of stainless steel balls and powder (gross power). Finally, the energy absorbed by milling media (net power) was derived from differences between the absorption of charged and empty vials. Fig. 9(a) shows the experimental results for Fe-Zr powder system. Full and open squares present measurement values for the absorp-

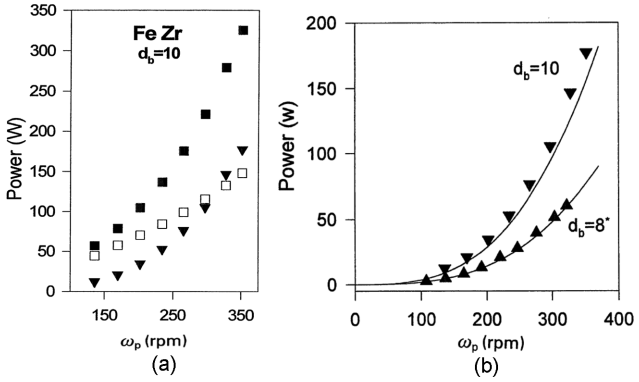

Fig. 9. (a) Electrical power absorption measured vs. the rotation speed of the mill for the Fe-Zr powder system [12] and (b) Experimental (full triangles) and calculated (full lines) power absorption for the Fe-Zr (99balls, d_b = 10, 40 g powder, BPR:10) and the Ti-Al (70 balls d_b= 8 + 13 balls d_b = 10, 20 g powder, BPR: 9.3) experiments [12].

tion of charged and empty vials, respectively. Full triangles give the net power, the power difference of the absorption of charged and empty vials (Fig. 9b).

The electrical power supplied to the milling device may be lost in a form of heat, friction, noise, etc. The measuring the absolute real values seemed to be impossible, so the electrical yield was assumed only the 80% of the measured values. With above assumption, the results show that the power consumption measured by the experiments is relatively well matched with the calculated one from the collision model.

5.5. Total energy transferred per unit weight of Powder (m_p) for a given milling time (t)

Eq. (4) describes that the energy is absorbed only by a small quantity of mass trapped in a collision but not by the total powders. We should take all the milling balls into account when considering the influence of ball-to-powder weight ratio. The total energy transferred per unit weight of powder (m_p) for a given milling time, t, can be expressed as

$$E_t = f_t \Delta E_b \times N_b t / m_p \,[\mathrm{J{\cdot}h/g}] \quad (10)$$

It must be pointed out that the energy given by Eq. (6) is not absorbed by the total powder and does not consider the influence of the ball number. So some researchers prefer to use $\Delta E_{b^*} - E_t$ energy map of Eq. (10) because all the milling parameters such as type of mill, type and size of ball, number of balls, rotation speed of the mill, ball to powder weight ratio, and milling time etc. can be converted simply into two energy parameters given above.

Murty *et al.* [29] set up a relationship between $\Delta E_{b^*} - E_t$ and ball-powder ratio or milling time to draw milling map of $Ti_{50}Ni_{50}$ and $Ti_{50}Cu_{50}$ as shown in Fig. 10 and Table 1, 2. This milling map clearly predicts a critical ΔE_b^* of 0.2J and a critical total energy, E_t, of 1.3 J·h/g. The milling map gives the milling conditions required for amorphization during mechanical alloying. This map can be taken as a glass formation map which can separate out the glass forming regime and the non-glass forming regime more or less distinctly. Thus, by knowing the above two parameters for a given composition and milling conditions one can predict the formation of amorphous phase from this energy map. Similar milling maps can be constructed for different alloy compositions. Fig. 10(b) is a milling map for $Ti_{50}Cu_{50}$ at two milling speeds with increasing milling time. The impact energy of the ball is fixed for a given milling speed in this case, while the total energy increases with increasing milling time as shown in Table 2. Even in this case amorphization was observed when the total energy is more than a critical value, 1.7 J·h/g.

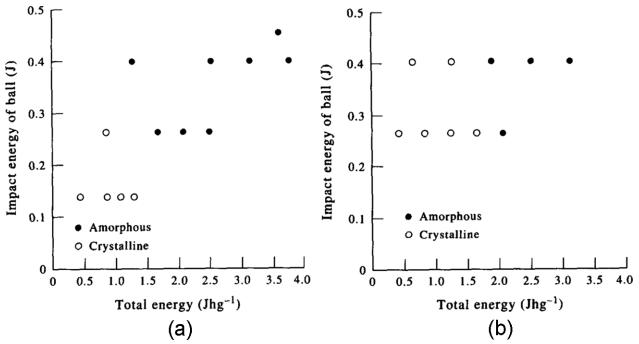

Fig. 10. (a) Milling map of $Ti_{50}Ni_{50}$ and (b) Milling map of $Ti_{50}Cu_{50}$.

Table 1. Energies of the balls at different milling intensities and ball to powder weight ratios for $Ti_{50}Ni_{50}$ (3 balls)

Milling intensity	E_b	E'_b	E_t^* for different weight ratios			
			4 : 1	8 : 1	10 : 1	12 : 1
4	0.14	0.137	0.426	0.852	1.065	1.278
6	0.27	0.264	0.821	1.641	2.052	2.463
8	0.41	0.401	1.247	2.493	3.117	3.742
9	0.47	0.459			3.567	

Table 2. Total milling energy for different durations of milling for $Ti_{50}Cu_{50}$ (3 balls)

Milling intensity	E_b	E'_b	E_t^* for different milling time (h)				
			4	8	12	16	20
6	0.27	0.264	0.821	1.641	2.052	2.463	2.052
8	0.41	0.401	1.247	2.493	3.117	3.742	3.117

The milling maps can be an adaptive method to correlate the milling conditions with the formation mechanism of various material systems recently reported. Rojacet *et al.* [26] used ball impact energy and cumulative kinetic energy to develop a milling map for $NaNbO_3$. Joardar *et al.* [30] established the milling criteria for the synthesis of nanocrystalline NiAl by mechanical alloying with changes in long-range order parameter at various milling energies. Abhik *et al.* [31] showed the variation of milling energy required for the start of formation of various compounds with their formation enthalpies. Singh

et al. [32] attempted to study effect of milling energy on the mechanical activation during the production of $MoSi_2$ form a reaction of Mo and Si_3N_4. Bhatt *et al.* [33] suggested that there is a common "energy window" for all the compositions in which amorphization is seen. But milling energies in excess of that required for the formation of amorphous phase will lead to in situ crystallization of the amorphous phase due to the raise in temperature during milling or due to large number of defects generated. Wu *et al.* [34] defined the energy region for the formation of nanocomposite WC-MgO powders. For the formation by gradual reaction in a long period, the specific energy of ball is low but the total energy is required double of SHS reaction.

6. Conclusion

1) From the collision model, energy transferred during planetary ball mill process can be calculated. $\Delta E_{b^*}-E_t$ energy map is preferred to use because all the milling parameters such as type of mill, type and size of ball, number of balls, rotation speed of the mill, ball to powder weight ratio, and milling time etc. can be converted simply into two energy parameters

2) Milling energy calculated from the collision model was in good agreement with the result from the measurement system of electrical power consumption during milling process.

3) Milling energy can be used for describing or predicting the relationship between process variables and the characteristics of end powder product, based on the theories. Milling maps with reaction(s) during milling process like amorphization or formation of intermetallics clearly supports this idea.

Acknowledgments

This work was supported by the National Research Foundation Grant funded by the Korean Government (NRF-2012R1A1A2044930).

References

[1] N. Burgio, A. Iasonna, M. Magini, S. Martelli and F. Padella: Nuovo Cimento, **13** (1991) 59.
[2] http://www.solid.nsc.ru/eng/develop/ago_eng.htm
[3] HEM/MA/RM-Devices in use, Modell nach: H. Zoz, 50 Aniversario de la Fundacion de la Esiqie, 3rd Intern. Symp. of THE SCHOOL OF CHEMICAL ENGINEERING, May 27-29, 1998.
[4] D. R. Maurice and T. H. Courtney: Metall. Trans. A, **21** (1990) 289-303.
[5] M. Magini: Mater. Sci. For., **121** (1992) 88.
[6] F. Padella, E. Paradise, N. Burgio, M. Magini, S. Martelli, W. Guo and A. Iasonna: Journal of the Less-Common Metals, **175** (1991) 79.
[7] P. Le Brun, L. Froyen and L. Delaey: Mater. Sci. Eng. A, **161** (1993) 75.
[8] E. Gaffet: Mater. Sci. Eng. A, **133** (1991) 181.
[9] M. Abdellaoui and E. Gaffet: Acta. Metall. Mater., **44** (1995) 1087.
[10] E. Gaffet, M. Abdellaoui and N. Malhouroux-Gaffet: Mater. Trans. JIM, **36** (1995) 198.
[11] D. Basset, P. Matteazzi and F. Miani: Mater. Sci. Eng. A, **174** (1994) 71.
[12] M. Magini and A. Iasonna: Mater. Trans. JIM, **36** (1995) 123.
[13] A. Iasonna and M. Magini: Acta mater., **44** (1996) 1109.
[14] M. Magini, C. Colella, A. Iasonna and F. Padella: Acta mater., **46** (1998) 2841.
[15] R. Watanabe, H. Hashimoto and G. G. Lee: Mater. Sci. Eng. A, **174** (1994) 71.
[16] Video introducing Pulverisette 6 classic line – FRITSCH GmbH, http://www.fritsch-milling.com/products/milling/planetary-mills/
[17] http://www.retsch.com/products/
[18] E. G. Avvakumov, A. R. Potkin and O. I. Samarin: Planetary mill. Author's certificate No. 975068, USSR, Patent Bulletin No. 43 (1982).
[19] http://www.fritsch-milling.com/products/milling/planetary-mills/pulverisette-7-premium-line/technical-data/
[20] M. Magini, A. Iasonna and F. Padella: Scripta metall. mat., **34** (1996) 13.
[21] P. P. Chattopadhyay, I. Manna, S. Talapatra and S. K. Pabi: Materials Chemistry and Physics, **68** (2001) 85.
[22] H. Mio, J. Kano, F. Saito and K. Kaneko: Mater. Sci. Eng. A, **332** (2002) 75.
[23] H. Mio, J. Kano, F. Saito and K. Kaneko: Int. J. Miner. Process., **74S** (2004) S85.
[24] H. Mio, J. Kano and F. Saito: Chemical Engineering Science, **59** (2004) 5909.
[25] S. Y. Lu, Q. J. Mao, Z. Peng, X. D. Li and J. H. Yan: Chin. Phys. B, **21** [7] (2012) 078201.
[26] T. Rojac, M. Kosec, B. Malic and J. Holc: Journal of the European Ceramic Society, **26** (2006) 3711.
[27] L. Liu and M. Magini: J. Mater. Res., **12** [9] (1997) 2281.
[28] H. A. Zhang and X. Y Liu: International Journal of Refractory Metals & Hard Materials, **19** (2001) 203.
[29] B. S. Murty, M. Mohan Rao and S. Ranganathan: Acta

Metall. Mater., **43** (1995) 2443.
[30] J. Joardar, S. K. Pabi and B. S. Murty: Journal of Alloys and Compounds, **429** (2007) 204.
[31] N. C. Abhik, R. Vivek, V. Udhayabanu and B. S. Murty: Journal of Alloys and Compounds, **465** (2008) 106.
[32] S. Singh, M. M. Godkhindi, R. V. Krishnarao and B. S. Murty: Journal of the European Ceramic Society, **29** (2009) 2069.
[33] J. Bhatt and B. S. Murty: Journal of Alloys and Compounds, **459** (2008) 135.
[34] C. X. Wu, S. G. Zhu, J. Ma and M. L. Zhang: Journal of Alloys and Compounds, **478** (2009) 615.